

Long-range order in the high-temperature phase of K_2ZnCl_4

F. X. Leduc, A. Hedoux, M. Descamps, F. Danede, and G. Odou

Laboratoire de Dynamique et Structure des Matériaux Moléculaires, URA 801, UFR de Physique, Bâtiment P5, Université de Lille 1, 59655 Villeneuve d'Ascq Cédex, France

(Received 17 March 1997)

X-ray-diffraction investigations of K_2ZnCl_4 reveal an ordered $ZnCl_4$ configuration that has a long-range-order character of the stable phase, through the observation of Bragg peaks located on the superstructure positions of the low-temperature phase, over the whole temperature range [110 K, 600 K], i.e., in the disordered phases ($T > 144$ K). The strong broadening of these superlattice reflections along \mathbf{a} above 144 K reveals a loss of the translational periodicity along \mathbf{a} and thus points out a strong one-dimensional distortion of the ordered state in the disordered phases. The phase transition into the ordered phase at 144 K is observed via an increasing of the low-temperature superstructure peaks at the high- Q values. At these \mathbf{Q} points an additional broad diffuse scattering was detected 50 K above the phase transition. The existence of the broad intensity can be interpreted from consideration of two different phenomena that could have the same origin: the disordered $ZnCl_4$ configuration generated by the relative sizes of the K cation and the rigid $ZnCl_4$ anion group. The behavior of the diffuse scattering was first interpreted in terms of local $ZnCl_4$ ordering, which could be a precursor of the phase transition at 144 K. A correlation between the $ZnCl_4$ ordering and the successive modulated-phase transitions is given from structural considerations. On the other hand, the diffuse scattering also could be the result of the defect structure that is responsible for the lattice distortion along the \mathbf{a} direction. [S0163-1829(97)04533-5]

I. INTRODUCTION

K_2ZnCl_4 is well known as an incommensurate insulator that undergoes the phase transition sequence (Table I) normal to incommensurate [$\mathbf{q}_\delta = \frac{1}{3}(1 - \delta)\mathbf{c}^*$] to commensurate ($\mathbf{q} = \mathbf{c}^*/3$), commonly observed in the various A_2BX_4 -type ferroelectrics. In contrast with the behavior of the prototype K_2SeO_4 , Zn compounds (Rb_2ZnCl_4 , K_2ZnCl_4 , Rb_2ZnBr_4 , etc.) do not exhibit a proper soft phonon and undergo supplementary modulated phases in the low-temperature range. In the A_2BX_4 family, the whole phase sequence is described from a prototypic hexagonal phase. Then the high-temperature orthorhombic phase of $Pm\bar{c}n$ symmetry can be interpreted as resulting from the hexagonal phase via small distortions. In the orthorhombic phase of the Zn compounds, BX_4 is disordered into two equivalent positions that are symmetry related with the m_a mirror in the $Pm\bar{c}n$ normal phase.¹ Consequently, the successive modulated phases can be interpreted as different steps in the BX_4 ordering process to reach the ordered monoclinic phase. This is in agreement with the structural description of the modulation in the incommensurate and commensurate phases, as rotations of BX_4 rigid

bodies around the \mathbf{b} and \mathbf{c} directions.²⁻⁴

Ab initio calculations show that the phase transitions in K_2SeO_4 ,⁵ K_2ZnCl_4 ,⁶ and Rb_2ZnCl_4 (Ref. 7) can be explained via a double-well structure in the potential-energy surfaces. On the top of the double well is the unstable $Pm\bar{c}n$ high-temperature phase, while at the bottom are two stable and ordered monoclinic phases. Both monoclinic phases correspond to two singlet ordered orientations of BX_4 , m_a symmetry related to each other and so have the same potential energy. The double well in K_2ZnCl_4 is deeper than that in Rb_2ZnCl_4 and much deeper than that in K_2SeO_4 . By decreasing the temperature, the compounds first transform to the higher entropy state, i.e., the incommensurate and commensurate phases, which are energetically quasiequivalent to the more stable phase. Second, by lowering the temperature further, the transformation into the monoclinic phase becomes more and more frustrated by the potential barrier. However, the calculated dispersion curves along [110] reveal that the boundary point $\mathbf{q} = (\mathbf{a}^* + \mathbf{b}^*)/2$ is unstable in Rb_2ZnCl_4 (Ref. 6) and K_2ZnCl_4 (Ref. 7) and so explains the observation of the monoclinic phase in both compounds. In addition, considerations on the behavior of calculated dispersion curves in

TABLE I. Description of the whole phase sequence in K_2ZnCl_4 , with the degree of the $ZnCl_4$ disorder that characterizes each phase.

Monoclinic 145 K $C1c1$	Orthorhombic 403 K $P2_1cn: \bar{1}s\bar{1}$	Orthorhombic 550 K $Pm\bar{c}n: ss\bar{1}$	T $Pm\bar{c}n$
$\frac{\mathbf{a}^* + \mathbf{b}^*}{2}$ commensurate phase	$\frac{\mathbf{C}^*}{3}$ commensurate phase	$(1 - \delta) \frac{\mathbf{c}^*}{3}$ incommensurate phase	Normal phase
one $ZnCl_4$ orientation	three $ZnCl_4$ orientations	infinite $ZnCl_4$ orientations	one average orientation

K_2ZnCl_4 (Ref. 7) suggest a possible observation of a soft optic mode that could be associated with a supplementary incommensurate phase [$\mathbf{q}_\delta = (\frac{1}{2} + \delta)\mathbf{a}^* + \frac{1}{2}\mathbf{b}^*$].

Controversial experiments were reported about this supplementary incommensurate phase in K_2ZnCl_4 . X-ray-diffraction experiments using synchrotron radiation⁸ have revealed no supplementary incommensurate phase, whereas an incommensurate modulation $\mathbf{q}_\delta = (\frac{1}{2} + \delta)\mathbf{a}^* + \frac{1}{2}\mathbf{b}^*$ was evidenced between 144 and 148 K from neutron-diffraction investigations.^{9,10} Nevertheless, inelastic neutron scattering experiments¹¹ performed on Rb_2ZnCl_4 and K_2ZnCl_4 show a special behavior of the soft optic branch [$\mathbf{q} = (\mathbf{a}^* + \mathbf{b}^*/2)$] in K_2ZnCl_4 and so point out an additional phenomenon to the first-order phase transition at 144 K. Different kinds of experiments (Raman spectroscopy,¹² x-ray diffraction,¹³ differential scanning calorimetry,^{12,13} and heat capacity measurements¹⁴) have pointed out a slow transformation of the $\mathbf{c}^*/3$ modulation, i.e., a slow ordering of ZnCl_4 tetrahedra. From x-ray investigations at the point (2.5, 1.5, 0) on a single crystal obtained from an evaporation of a $\text{ZnCl}_2 + \text{KCl}$ solution that was not drastically controlled, this transformation was associated with the development of the diffuse scattering observed at the superstructure position [$\mathbf{q} = (\mathbf{a}^* + \mathbf{b}^*)/2$] of the monoclinic phase. Two phenomena are clearly evident: the development of the broad diffuse scattering observed about 50 K above the phase transition at 144 K and the merging of the $\mathbf{q} = (\mathbf{a}^* + \mathbf{b}^*)/2$ superlattice reflection at 144 K.

From all investigations on K_2ZnCl_4 it can be assumed that the development of the diffuse scattering should be a precursor to the ordered ZnCl_4 arrangement at 144 K. To give a better insight of the ordering process of the tetrahedra, x-ray investigations at the superlattice points $\mathbf{q} = (\mathbf{a}^* + \mathbf{b}^*)/2$ were extended to a wide Q range.

II. EXPERIMENT

X-ray-diffraction experiments were carried out on a four-circle diffractometer, using a Huber goniometer and driving software developed in house. This device is well adapted to the study of modulated structures and allows us to record data collection through different methods: θ scans, θ - 2θ scans, and Q scans. The last method was used to study the $(\mathbf{a}^* + \mathbf{b}^*)/2$ superstructure lines in the Q range ($0.140 \leq 2 \sin \theta/\lambda \leq 0.640$). The diffractometer equipment used Mo $K\alpha$ radiation ($\lambda = 0.7107 \text{ \AA}$) and so the measured half-width at half maximum (HWHM) of the superstructure reflections were obtained from correction with Rachinger method. The intrinsic broadening of superlattice reflections were obtained from the measured HWHM $\Delta^m Q$ corrected by the experimental resolution $\Delta^R Q$ as¹⁵

$$\Delta Q = [(\Delta^m Q)^2 - (\Delta^R Q)^2]^{1/2}.$$

The experimental resolution was determined for a given superstructure line from the HWHM of a neighboring reflection in the reference crystal (CaF_2). The typical size of the quasispherical single crystals was $\varnothing = 0.5 \text{ mm}$. Investigations were conducted in the temperature range 110–650 K.

The single crystals are obtained by slow cooling of an aqueous solution. A germ of K_2ZnCl_4 was inserted in a satu-

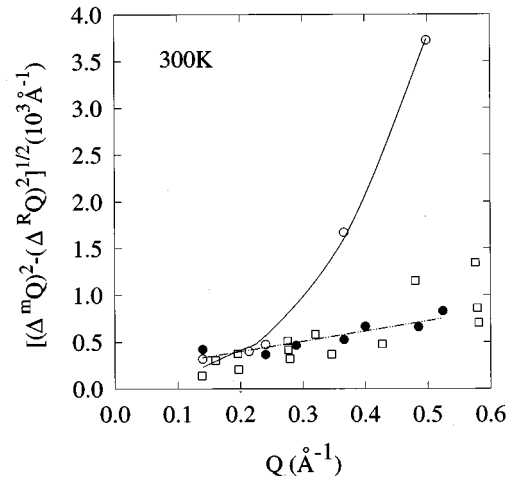


FIG. 1. Q dependence of the HWHM at 300 K of the low-temperature superlattice reflections from Q scans along \mathbf{a}^* (open circles) and along \mathbf{b}^* (full circles), and of the fundamental Bragg peaks from Q scans along \mathbf{a}^* (open squares).

rated aqueous solution ZnCl_2 - KCl in stoichiometric proportions, at 303 K. The temperature was slowly decreased (0.1 K/day) and four months later a 2.8-g single crystal was obtained. All the samples used in the reported experiments were prepared from this single crystal.

III. RESULTS

The $(\mathbf{a}^* + \mathbf{b}^*)/2$ points of the reciprocal lattice were scanned along the \mathbf{a}^* and \mathbf{b}^* directions at room temperature for several Q values in the accessible Q range on an as-grown sample. A striking feature is the observation of peaks located in the low-temperature superstructure positions. These peaks are well fitted by a Gaussian line shape. The fittings show a strong Q dependence along the \mathbf{a}^* direction of the HWHM ($\Delta Q \propto Q^n$ with $n > 2$) for the high- Q values (Fig. 1), whereas the peak intensity decreases with Q as the result of the lost periodicity along \mathbf{a} . The fundamental Bragg reflections were also analyzed and exhibit a weak broadening along \mathbf{a} versus Q .

Investigations in the high-temperature range [300 K, 600 K] reveal that the superstructure lines of the low-temperature phase are observed even in the high-temperature phase for the low- Q values (Fig. 2). These results suggest the existence of a long-range-ordered state in the nonordered commensurate, incommensurate, and normal phases. However, the ordered state does not exhibit a periodic arrangement along \mathbf{a} , in contrast to the disordered state corresponding to the fundamental Bragg reflections of the average structure.

Investigations in the low-temperature range [110 K, 300 K] show a weak temperature dependence of the $(\mathbf{a}^* + \mathbf{b}^*)/2$ superstructure lines down to 144 K (Fig. 3). The phase transition into the ordered monoclinic phase is characterized by a strong increase in the integrated intensity of the superstructure lines, connected with a considerable sharpening (Table II), only for the high- Q values ($Q \geq 0.37 \text{ \AA}^{-1}$), whereas no change is observed for the peak at the lowest- Q value (Figs. 3 and 4). Consequently, it can be assumed that the phase transition at 144 K generates a more homoge-

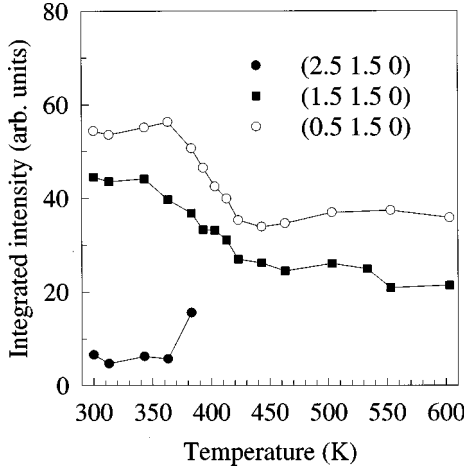


FIG. 2. Temperature dependence of the integrated intensity of the low-temperature superstructure reflections in the high-temperature range.

neous arrangement of the ordered ZnCl_4 configuration along **a**.

At the $(\mathbf{a}^* + \mathbf{b}^*)/2$ points, an additional broad diffuse scattering is observed along \mathbf{a}^* , only for the high- Q values ($Q \geq 0.37 \text{ \AA}^{-1}$), from about 200 K down to 144 K (Fig. 4). The diffuse scattering is well fitted using a Lorentzian profile. The full width at half maximum (FWHM) is plotted as a function of the temperature (Fig. 5) for two different points: (2.5, 1.5, 0) and (3.5, 1.5, 0). As observed on Figs. 4 and 5, the integrated intensity of the diffuse scattering increases by lowering the temperature and decreases suddenly to zero below the phase transition, i.e., when the intensity of the superstructure peak increases greatly (below $T = 145 \text{ K}$).

To describe the ordering process of ZnCl_4 tetrahedra, i.e., the growing process of the ordered monoclinic phase, the x-ray scattering intensity located at the $\mathbf{q} = (\mathbf{a}^* + \mathbf{b}^*)/2$ points of the reciprocal lattice was analyzed as explained below. The intensity is given by¹⁶

$$S(\mathbf{Q}, T) \propto \text{tr} \left\| \bar{F}(\mathbf{Q}) \cdot \bar{\chi}(\mathbf{Q}, T) \right\|,$$

where $F^{\alpha\beta}(\mathbf{Q}) = f_{\alpha}(\mathbf{Q})f_{\beta}^*(\mathbf{Q})$, $f_i(\mathbf{Q})$ being the molecular x-ray form factors of the molecule in the different possible orientations, and $\bar{\chi}(\mathbf{Q}, T)$ is the susceptibility matrix; its elements are the Fourier transform of the correlation functions

$$G_{\alpha\beta}(\mathbf{r}, T) = \langle \mu_{\alpha}(0, T) \mu_{\beta}(\mathbf{r}, T) \rangle - \langle \mu_{\alpha}(0, T) \rangle \langle \mu_{\beta}(\mathbf{r}, T) \rangle,$$

where $\mu_{\alpha}(\mathbf{r}, T)$ specifies the orientation at site \mathbf{r} and temperature T .

TABLE II. Experimental determination of the broadening of the low-temperature superlattice reflections versus Q above (300 K) and below (128 K) the phase transition at 144 K.

$\left(\frac{\mathbf{a}^* + \mathbf{b}^*}{2}\right)$ reflections	ΔQ ($\text{\AA}^{-1} \times 10^3$) 300 K	ΔQ ($\text{\AA}^{-1} \times 10^3$) 128 K
(0.5, 1.5, 0)	0.255(7)	0.245(3)
(1.5, 1.5, 0)	0.59(1)	0.52(1)
(2.5, 1.5, 0)	1.72(2)	0.53(1)
(3.5, 1.5, 0)	3.74(9)	3.32(2)

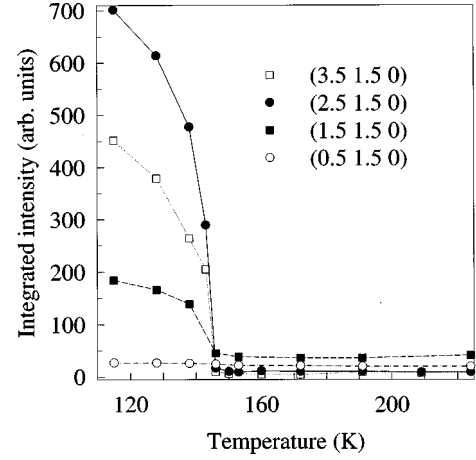


FIG. 3. Temperature dependence of the integrated intensity of the low-temperature superstructure reflections in the low-temperature range.

To interpret the Lorentzian line shape of the diffuse scattering, a local ordering model described by an Ornstein-Zernike correlation function $G(\mathbf{r}, T)$ is used. Assuming the description of the orientations with an Ising model 1/2, $\langle \mu_0 \mu_r \rangle$ is given by¹⁷

$$\frac{\exp\left(\frac{-2r}{L(T)}\right)}{r},$$

where $L(T)/2$ is the correlation length at the temperature T . Consequently,

$$G(\mathbf{r}, T) = \frac{\exp\left[\frac{-2r}{L(T)}\right]}{r}$$

and

$$S(\mathbf{q}, T) = \frac{1}{\left(\frac{1}{L(T)}\right)^2 + (\pi q)^2}$$

gives the line shape of the scattering intensity. In this case the HWHM Γ (reciprocal lattice unit) is a fitted parameter of the Lorentzian line shape that is directly correlated to the characteristic size L (lattice unit) by

$$L(T) = \frac{1}{\pi} \Gamma^{-1}(T).$$

Writing the susceptibility as a function of $qL(T)$,

$$S(\mathbf{q}, T) = L^2(T) \hat{S}(\pi q L(T)),$$

it can be predicted by a scaling law (I versus Γ^{-1}), with exponent $x=2$, to characterize the development of the diffuse scattering.

The log-log plot of the peak intensity versus Γ^{-1} points out, by fitting with a first-order regression, a scaling exponent $x \approx 2$ (Fig. 6). This result shows a continuous and homogeneous ZnCl_4 local ordering within microclusters characterized by a correlation length $L(T > 150 \text{ K}) \approx 30 \text{ \AA}$. The

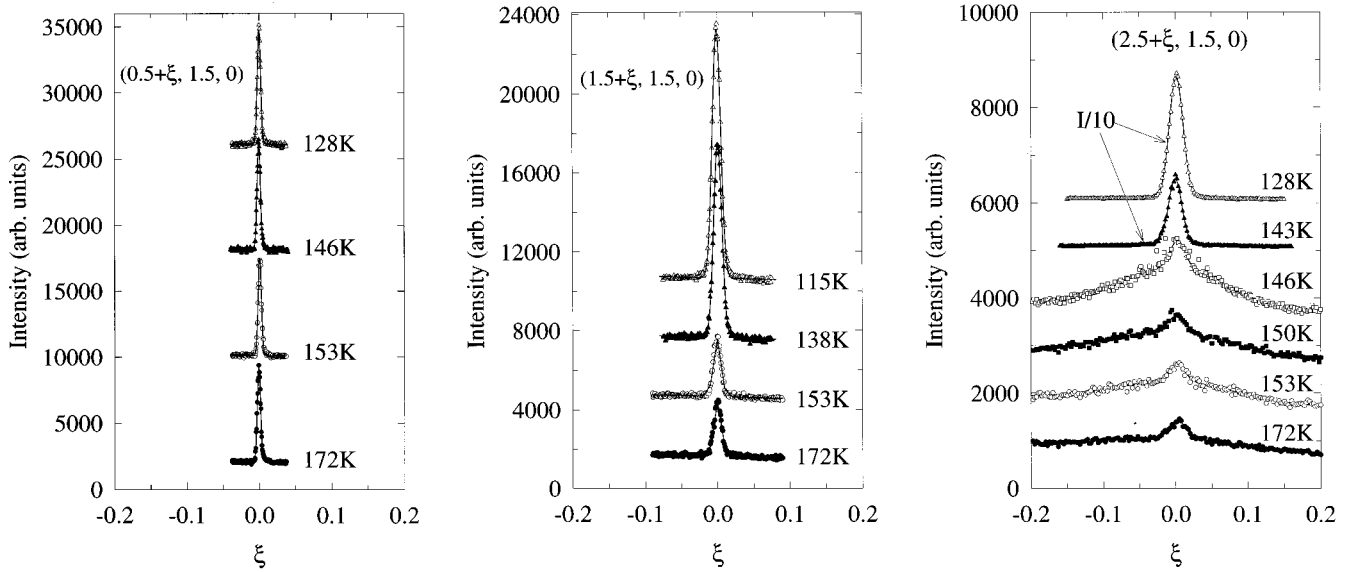


FIG. 4. Temperature dependence of the Q scans along \mathbf{a}^* of the low-temperature superstructure reflections for different Q values, in (a) $(0.5, 1.5, 0)$, (b) $(1.5, 1.5, 0)$, and (c) $(2.5, 1.5, 0)$, scaled in Q to give a better observation of the broadening along \mathbf{a}^* .

inverse susceptibility T/I exhibits a linear T dependence (Fig. 7), as expected from the Landau theory. Consequently, the structure of the commensurate, incommensurate, and normal phases should be described by disordered domains embedded within a long-range-ordered matrix. From x-ray experiments, the ZnCl_4 ordering in the disordered domains should start from about 200 K, where the broad intensity was detected.

On the other hand, the diffuse intensity could result from the defect structure that is responsible for the lattice distortion along \mathbf{a} . The inhomogeneous arrangement of ordered ferroelectric domains could generate strains between ordered domains. The broadened intensity should be assigned to a Huang-type scattering.^{18–20} The detection of the broadened intensity, only at the high- Q values, should corroborate this hypothesis because of the Q^2 dependence of the Huang scattering intensity.

IV. DISCUSSION

The first feature of this study is the experimental evidence of a long-range-ordered state in the disordered, incommensurate, commensurate, and normal phases. This observation should indicate a long-range correlation between the rotations of ZnCl_4 tetrahedra around their ordered orientation. The lack of the translational periodicity that is principally observed along \mathbf{a} can be assigned to an inhomogeneous arrangement of ordered ferroelectric domains. Two kinds of ferroelectric domains can be observed in K_2ZnCl_4 because of the existence of two ferroelectric phases.

The $\mathbf{c}^*/3$ ferroelectric domains are generally observed in the soliton regime, i.e., in the incommensurate phase, only a few degrees above the lock-in phase transition with decreasing temperature. The modulation has a commensurate periodicity $\mathbf{c}^*/3$, whereas the domain walls are characterized by an incommensurate modulation $(1-\delta)\mathbf{c}^*/3$ and thus they are called discommensurations. Electron microscopy experiments^{21,22} show that the incommensurate-

commensurate phase transition corresponds to nucleation and annihilation processes of discommensurations that move

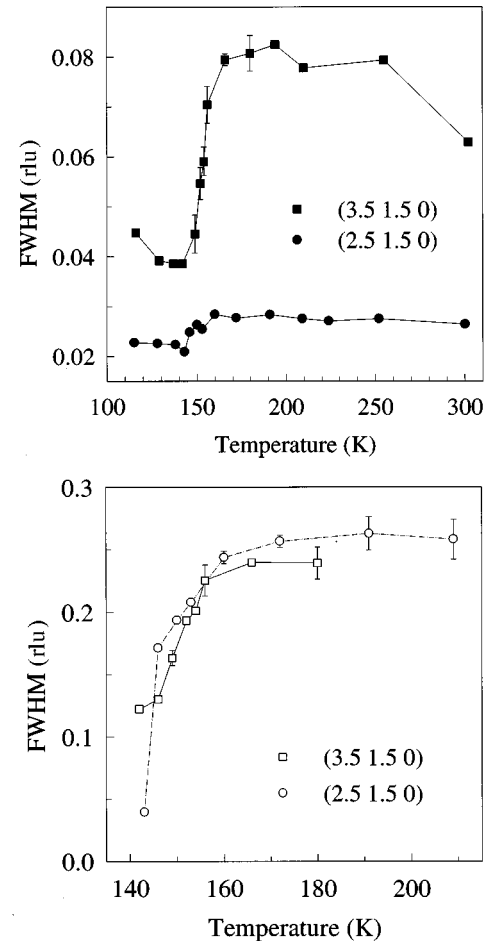


FIG. 5. Temperature dependence of the FWHM corresponding to (a) the $(\mathbf{a}^* + \mathbf{b}^*)/2$ superlattice reflections and (b) the diffuse scattering observed on the same $(\mathbf{a}^* + \mathbf{b}^*)/2$ points in the high- Q range.

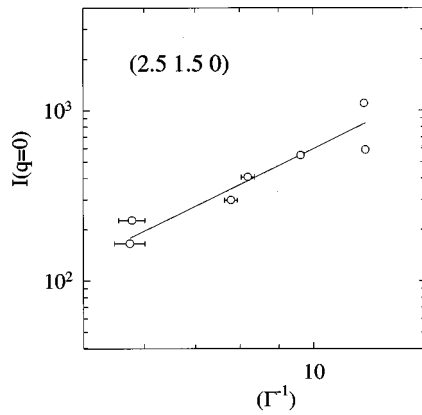


FIG. 6. The log-log plot of the (2.5, 1.5, 0) diffuse scattering intensity versus the inverse width Γ^{-1} .

along the \mathbf{a} direction. Consequently, the phase-transition process is connected to the concentration and the mobility of the discommensurations. Different studies^{22,23} have revealed a high concentration and an inhomogeneous arrangement of discommensurations at room temperature in K_2ZnCl_4 . These observations should have a contribution to the broadening of the $(\mathbf{a}^* + \mathbf{b}^*)/2$ superlattice reflections along \mathbf{a} .

The second feature is the observation of a broad diffuse intensity distribution along \mathbf{a}^* , only on the points corresponding to the superstructure peaks that exhibit a strong temperature dependence of intensity and a FWHM at 144 K. Figure 7 shows the critical behavior of the ZnCl_4 ordering at the point $\mathbf{q} = (\mathbf{a}^* + \mathbf{b}^*)/2$. The temperature dependence of the diffuse scattering can be interpreted from the consideration of two phenomena.

(i) The local ZnCl_4 ordering should be responsible for the observation of the broad diffuse intensity and thus the development of the diffuse scattering would be a precursor to the phase transition at 144 K. This phase transition is associated with the softening of an optical mode¹¹ that exhibits a minimum in the $\mu\mathbf{a}^* + \frac{1}{2}\mathbf{b}^*$ direction. This phenomenon should correlate with a quasielastic component, interpreted as a ZnCl_4 ordering involved in the phase transition. This inter-

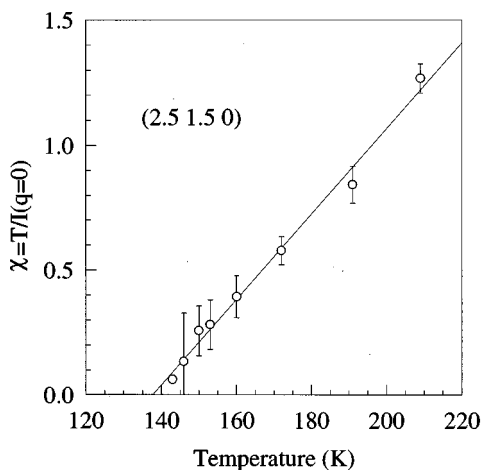


FIG. 7. Plot of the linear temperature dependence of the susceptibility for the diffuse scattering measured at (2.5, 1.5, 0).

pretation is in agreement with previous spectroscopy and calorimetry.

(ii) The inhomogeneous arrangement of the $(\mathbf{a}^* + \mathbf{b}^*)/2$ ferroelectric domain that are responsible for the broadening of the $(\mathbf{a}^* + \mathbf{b}^*)/2$ superlattice reflections could generate strains between domains and thus give rise to a temperature-dependent diffuse scattering.

Both hypotheses should be a consequence of a disorder generated by a smaller size of the K cations compared to the size of the ZnCl_4 anions.^{24,25} This size criterion should also be responsible for the existence of the incommensurate lattice instability in the $A_2\text{BX}_4$ compounds. This phenomenon is in agreement with the hypothesis that the ordered phase is due to the softening of modes that were soft in the prototypic hexagonal high-temperature phase.¹¹

From the present study, the phase transition at 144 K is interpreted in terms of rearrangement of the $(\mathbf{a}^* + \mathbf{b}^*)/2$ ferroelectric domains into a more homogeneous distribution along the \mathbf{a} direction. The ordered ferroelectric state appears as a stable ZnCl_4 configuration over the whole temperature range. The rearrangement of the low-temperature domains was performed either via a local ZnCl_4 ordering or via strains between domains that involve the ferroelastic distortion at 144 K (Table I).

This study reveals also two different defects of periodicity. The incommensurate phase of K_2ZnCl_4 corresponds to a lack of periodicity along the \mathbf{c} direction. However, the satellite reflections exhibit no broadening versus Q . On the other hand, the loss of periodicity along the \mathbf{a} direction is characterized by a broadening of the $(\mathbf{a}^* + \mathbf{b}^*)/2$ superlattice reflections. This phenomenon can be explained from the consideration that the \mathbf{a} direction is soft.

From the structural study of the modulated phases of Rb_2ZnCl_4 (Ref. 2) and K_2ZnCl_4 ,³ the modulation is principally described as rotations of ZnCl_4 rigid groups around the pseudo-hexagonal \mathbf{c} axis, corresponding to the largest modulated displacements of Cl atoms along the \mathbf{a} direction. These considerations can explain the inhomogeneous ordered ZnCl_4 configuration along \mathbf{a} , at room temperature (in the commensurate phase), and the diffuse scattering along \mathbf{a} should correspond principally to the rearrangement of Cl atoms along the \mathbf{a} direction.

In a previous study³ performed on single crystals characterized by a poor crystal-growth quality, the diffuse scattering was observed from 250 K and the superstructure peak (2.5, 1.5, 0) was not observed above 144 K. This can be interpreted by a more inhomogeneous arrangement of the $(\mathbf{a}^* + \mathbf{b}^*)/2$ ferroelectric domains above 144 K, which involves either a more important local ordering or stronger strains between the low-temperature domains. The extreme difficulty in obtaining a periodic arrangement of $(\mathbf{a}^* + \mathbf{b}^*)/2$ ferroelectric domains can be assigned to the interaction between the $\mathbf{c}^*/3$ modulation and the crystal-growth defects. This phenomenon is closely connected to the stability of the incommensurate and commensurate modulated phases.^{26,27} The ZnCl_4 orientations are pinned to the defects and thus the stability of the modulated phase (incommensurate or commensurate) is increased. It was observed³ that a slower crystal growth generates a larger coherence length of

the ordered ZnCl_4 configuration at the temperature of the crystal growth. As a consequence, the crystal-growth quality is closely connected to the ZnCl_4 ordering in K_2ZnCl_4 certainly in relation to the high degree of disorder of the ZnCl_4

tetrahedra generated by the relative sizes of K and ZnCl_4 . These considerations can explain why the development of the diffuse scattering along \mathbf{a}^* above the low-temperature phase is observed only in K_2ZnCl_4 .

-
- ¹K. Itoh, A. Hinasada, H. Matsunaga, and E. Nakamura, *J. Phys. Soc. Jpn.* **52**, 664 (1983).
- ²A. Hedoux, D. Grebille, J. Jaud, and G. Godefroy, *Acta Crystallogr. Sec. B* **45**, 370 (1989).
- ³M. Quilichini, P. Bernede, J. Lefebvre, and P. Schweiss, *J. Phys. Condens. Matter* **2**, 4543 (1990).
- ⁴A. C. R. Hogervorst and R. B. Helmhodt, *Acta Crystallogr. Sec. B* **44**, 120 (1988).
- ⁵H. M. Lu and J. R. Hardy, *Phys. Rev. Lett.* **64**, 661 (1990).
- ⁶P. J. Edwardson, V. Katkanan, and J. R. Hardy, *Phys. Rev. B* **35**, 8470 (1987).
- ⁷H. M. Lu and J. R. Hardy, *Phys. Rev. B* **46**, 8582 (1992).
- ⁸K. Hasebe, T. Asahi, H. Kasano, H. Mashiyama, and S. Kishimoto, *J. Phys. Soc. Jpn.* **63**, 3340 (1994).
- ⁹K. Gesi, *J. Phys. Soc. Jpn.* **59**, 416 (1990).
- ¹⁰K. Gesi, *J. Phys. Soc. Jpn.* **61**, 1225 (1992).
- ¹¹M. Quilichini, V. Dvorak, and P. Boutrouille, *J. Phys. (France) I* **1**, 1321 (1991).
- ¹²I. Noiret, A. Hedoux, Y. Guinet, and M. Foulon, *Europhys. Lett.* **22**, 265 (1993).
- ¹³A. Hedoux, Y. Guinet, F. X. Leduc, M. More, M. Foulon, F. Danede, and G. Odou, *J. Phys. Condens. Matter* **7**, 7651 (1995).
- ¹⁴J. C. Van Miltenburg, I. Noiret, and A. Hedoux, *Thermochim. Acta* **239**, 33 (1994).
- ¹⁵R. Moret, J. P. Pouget, R. Comès, and K. Bechgaard, *J. Phys. (France)* **46**, 1521 (1985).
- ¹⁶M. Descamps, *J. Phys. C* **15**, 7265 (1982).
- ¹⁷H. E. Stanley, *Introduction to Phase Transition and Critical Phenomena* (Clarendon, Oxford, 1971).
- ¹⁸K. Huang, *Proc. R. Soc. London, Ser. A* **190**, 102 (1947).
- ¹⁹P. H. Dederichs, *J. Phys. F* **3**, 471 (1973).
- ²⁰O. Blaschko, W. Schwarz, W. Schranz, and A. Fuith, *J. Phys. Condens. Matter* **6**, 3469 (1994).
- ²¹H. Sakata, K. Hamano, X. Pan, and H. G. Unruh, *J. Phys. Soc. Jpn.* **59**, 1079 (1990).
- ²²X. Pan and H. G. Unruh, *J. Phys. Condens. Matter* **2**, 323 (1990).
- ²³F. X. Leduc, A. Hédoux, Y. Guinet, F. Danede, G. Odou, and M. More, *Ferroelectrics* **185**, 229 (1996).
- ²⁴J. M. Perez-Mato, I. Etxebarria, and G. Madariaga, *Phys. Scr.* **T39**, 81 (1991).
- ²⁵I. Etxebarria, J. M. Perez-Mato, and Madariaga, *Phys. Rev. B* **46**, 2764 (1991).
- ²⁶A. Hedoux, D. Grebille, J. Lefebvre, and R. Perret, *Phase Transit.* **14**, 177 (1989).
- ²⁷I. Noiret, A. Hedoux, Y. Guinet, and F. X. Leduc, *J. Phys. Condens. Matter* **7**, 413 (1995).